

UNIVERSIDAD SAN FRANCISCO DE QUITO USFQ

Colegio de Ciencias e Ingenierías

Evaluación Teórica de *rccc* R-Pirogalol[4]arenos Funcionalizados con Metales como Medio para el Almacenamiento de Hidrógeno Molecular

Ensayos o Artículos Académicos

Víctor H. Posligua

Ingeniería Química

Trabajo de titulación presentado como requisito
para la obtención del título de
Ingeniero Químico

Quito, 17 de diciembre de 2015

UNIVERSIDAD SAN FRANCISCO DE QUITO USFQ
COLEGIO DE CIENCIAS E INGENIERÍAS

HOJA DE CALIFICACIÓN
DE TRABAJO DE TITULACIÓN

**Evaluación Teórica de *rccc* R-Pirogalol[4]arenos Funcionalizados con Metales
como Medio para el Almacenamiento de Hidrógeno Molecular**

Víctor H. Posligua

Calificación:

Nombre del profesor, Título académico

F. Javier Torres, Ph.D.

Firma del profesor

Quito, 17 de diciembre de 2015

Derechos de Autor

Por medio del presente documento certifico que he leído todas las Políticas y Manuales de la Universidad San Francisco de Quito USFQ, incluyendo la Política de Propiedad Intelectual USFQ, y estoy de acuerdo con su contenido, por lo que los derechos de propiedad intelectual del presente trabajo quedan sujetos a lo dispuesto en esas Políticas.

Asimismo, autorizo a la USFQ para que realice la digitalización y publicación de este trabajo en el repositorio virtual, de conformidad a lo dispuesto en el Art. 144 de la Ley Orgánica de Educación Superior.

Firma del estudiante: _____

Nombres y apellidos: Víctor Hugo Posligua Hernández

Código: 00121319

Cédula de Identidad: 171551495-4

Lugar y fecha: Quito, 17 de diciembre de 2015

RESUMEN

En el presente estudio se reporta la investigación teórica acerca del potencial de los pirogalol[4]arenos R-sustituidos funcionalizados con varios metales (M-R-Pyg[4]arenos; M = Li⁺, K⁺, Na⁺ y Mg²⁺; R = meil y fluoretil) como medio para el almacenamiento de hidrógeno molecular (H₂). Como punto de partida, las características estructurales de los sistemas funcionalizados con los metales fueron obtenidos al nivel de teoría B3LYP/6-311G(d,p). Subsecuentemente, la interacción de la molécula de hidrógeno con los cationes integrados en la cavidad de las moléculas macrocíclicas es descrita con el funcional B3LYP usando dos conjuntos base de diferente flexibilidad, BSA: 6-311G(d,p) para todos los átomos, y BSB: 6-311G(d,p) y aug-cc-pVDZ para M-R-Pyg[4]arenos e H₂, respectivamente. Los valores obtenidos de las energías de amarre corregidas por el método BSE usando el nivel de teoría B3LYP/BSB fueron notablemente más altas para los complejos H₂/M-R-Pyg[4]areno abarcando el rango entre 1.3 y 17.0 kJ/mol. Estos resultados fueron posteriormente refinados mediante dos aproximaciones: (i) empleando el funcional B97D, el mismo que incluye una corrección de tipo Grimme para la descripción de las fuerzas de dispersión y (ii) realizando cálculos MP2 mediante la utilización del método ONIOM. Las energías de amarre resultantes, usando el nivel MP2, mostraron un incremento de aproximadamente 2.5 kJ/mol al analizar a todos los complejos. Por otra parte, se encontró que las energías de amarre obtenidas usando B97D muestran valores sobrestimados debido a que se evidenciaron incrementos considerablemente grandes (el triple y el cuádruple de los valores obtenidos mediante B3LYP para los casos de los sistemas funcionalizados con Li y Na, respectivamente). Para el caso específico del H₂/fluoretil-Pyg[4]areno, la entalpía de adsorción estimada (ΔH°_{ads}) fue de -17.6 kJ/mol tomando en cuenta la energía del punto cero (ZPE) y los efectos térmicos calculados a 300 K a partir de las frecuencias armónicas vibracionales obtenidas al nivel de teoría B3LYP/BSB. Esta entalpía de adsorción alta sugiere que los R-Pyg[4]arenos funcionalizados con Mg pueden ser tomados en cuenta como sistemas prometedores para el almacenamiento de hidrógeno molecular.

Palabras clave: DFT, Pirogalol, Macrociclos, Almacenamiento de H₂, Fuerzas de dispersión, Adsorción.

ABSTRACT

In the present study, a theoretical investigation of the potential of various metal-functionalized R-substituted pyrogallol[4]arenes (i.e., M-R-Pyg[4]arene; M = Li⁺, K⁺, Na⁺ and Mg²⁺; R = methyl and fluoroethyl) as media for molecular hydrogen (H₂) storage is reported. Initially, the structural features of the metal-functionalized systems are obtained at the B3LYP/6-311G(d,p) level of theory. Subsequently, the interaction of a H₂ molecule with the cations embedded in the cavity of the macrocyclic molecules is described with the B3LYP functional using two basis sets of different flexibility, namely BSA: 6-311G(d,p) for all atoms, and BSB: 6-311G(d,p) and aug-cc-pVDZ for M-R-Pyg[4]arene and H₂, respectively. Notably large BSSE-corrected binding energy values were obtained at the B3LYP/BSB level for the different H₂/M-R-Pyg[4]arene complexes spanning the 1.3 – 17.0 kJ/mol range. The resulting values were further refined through two approaches: (i) by employing the functional B97D, which includes a Grimme's type correction for describing dispersive forces and (ii) by performing MP2 calculations within the frame of the ONIOM approach. Binding energies refined at the MP2 level resulted in an average increment of about ~2.5 kJ/mol when considering all the complexes under investigation. On the other hand, B97D binding energies were found to be overestimated since too large increments (i.e., three- and fourfold with respect to B3LYP values for the case of Li- and Na-functionalized systems, respectively) were observed. For the specific case of the H₂/Mg-fluoroethyl-Pyg[4]arene, an adsorption enthalpy ($\Delta H^{\circ}_{\text{ads}}$) of -17.6 kJ/mol was estimated by adding the zero point energy and thermal effects computed at 300 K from harmonic vibrational frequencies, obtained at the B3LYP/BSB level. This relatively high adsorption enthalpy suggests that Mg-functionalized R-Pyg[4]arenes can be envisaged as promising systems for molecular hydrogen storage.

Keywords: DFT, Pyrogallol, Macrocycles, H₂ storage, Dispersive forces, Adsorption.

TABLA DE CONTENIDO

1. Introducción.....	9
2. Modelos y métodos.....	10
3. Resultados y discusión.....	12
3.1 Descripción geométrica de M-R-Pyg[4]arenos.....	12
3.2 Interacción del H₂ con M-R-Pyg[4]arenos.....	13
3.3 Inclusión de fuerzas de dispersión.....	14
4. Conclusiones.....	15
Agradecimientos.....	16
Referencias.....	16

ÍNDICE DE TABLAS

Tabla 1. Características geométricas de los R-Pyg[4]arenos funcionalizados con metales optimizados al nivel de teoría B3LYP/6-311G(d,p).....	12
Tabla 2. Características geométricas, energías de amarre con y sin corrección BSSE (BE y BE ^C respectivamente) de los complejos H ₂ /M-R-Pyg[4]arenos optimizados a niveles de teoría B3LYP/BSA y B3LYP/BSB.....	14
Tabla 3. Energías de amarre con y sin corrección BSSE (BE y BE ^C respectivamente) calculadas para los diferentes complejos H ₂ /M-R-Pyg[4]areno empleando el funcional B97D y el método ONIOM con conjuntos base BSA y BSB.....	14

ÍNDICE DE FIGURAS

- Figura 1.** Representación esquemática de la conformación en forma de copa de pirogalol[4]arenos R-sustituidos (*rccc*-R-Pyg[4]arenos).....11
- Figura 2.** Entorno local de un catión incrustado en la cavidad de un *rccc*-R-Pyg[4]areno.....13
- Figura 3.** Porción de átomos de los complejos H₂/M-R-Pyg[4]areno empleados como sistema modelo en los cálculos ONIOM del presente trabajo.....15



Contents lists available at ScienceDirect

Computational and Theoretical Chemistry

journal homepage: www.elsevier.com/locate/comptcTheoretical evaluation of metal-functionalized *rccc* R-pyrogallol[4] arenes as media for molecular hydrogen storageV. Posligua^{a,b}, A.S. Urbina^{a,b}, L. Rincón^{a,c}, J.-C. Soetens^d, M.A. Méndez^{a,b,e}, C.H. Zambrano^{a,b}, F.J. Torres^{a,b,d,*}^a Universidad San Francisco de Quito, Grupo de Química Computacional y Teórica (QCT-USFQ), Departamento de Ingeniería Química, Diego de Robles y Vía Interoceánica, Quito 17-1200-841, Ecuador^b Universidad San Francisco de Quito, Grupo Ecuatoriano para el Estudio Experimental y Teórico de Nanosistemas (GETNano), Diego de Robles y Vía Interoceánica, Quito 17-1200-841, Ecuador^c Departamento de Química, Facultad de Ciencias, Universidad de Los Andes, La Hechicera, Mérida 5101, Venezuela^d Université de Bordeaux, ISM, UMR 5255, 351, Cours de la Libération, Talence F-33405, France^e Universidad San Francisco de Quito, Colegio de Ciencias de la Salud, Edificio de Especialidades Médicas, Hospital de los Valles, Av. Interoceánica Km 12 ½, Quito, Ecuador

ARTICLE INFO

Article history:

Received 18 July 2015

Received in revised form 27 August 2015

Accepted 28 August 2015

Available online 11 September 2015

Keywords:

DFT

Pyrogallol

Macrocycles

H₂ storage

Dispersive forces

Adsorption

ABSTRACT

In the present study, a theoretical investigation of the potential of various metal-functionalized R-substituted pyrogallol[4]arenes (i.e., M-R-Pyg[4]arene; M = Li⁺, K⁺, Na⁺ and Mg²⁺; R = methyl and fluoroethyl) as media for molecular hydrogen (H₂) storage is reported. Initially, the structural features of the metal-functionalized systems are obtained at the B3LYP/6-311G(d,p) level of theory. Subsequently, the interaction of a H₂ molecule with the cations embedded in the cavity of the macrocyclic molecules is described with the B3LYP functional using two basis sets of different flexibility, namely BSA: 6-311G(d,p) for all atoms, and BSB: 6-311G(d,p) and aug-cc-pVDZ for M-R-Pyg[4]arene and H₂, respectively. Notably large BSSE-corrected binding energy values were obtained at the B3LYP/BSB level for the different H₂/M-R-Pyg[4]arene complexes spanning the 1.3–17.0 kJ/mol range. The resulting values were further refined through two approaches: (i) by employing the functional B97D, which includes a Grimme's type correction for describing dispersive forces and (ii) by performing MP2 calculations within the frame of the ONIOM approach. Binding energies refined at the MP2 level resulted in an average increment of about ~2.5 kJ/mol when considering all the complexes under investigation. On the other hand, B97D binding energies were found to be overestimated since too large increments (i.e., three- and fourfold with respect to B3LYP values for the case of Li- and Na-functionalized systems, respectively) were observed. For the specific case of the H₂/Mg-fluoroethyl-Pyg[4]arene, an adsorption enthalpy (ΔH_{ads}^0) of −17.6 kJ/mol was estimated by adding the zero point energy and thermal effects computed at 300 K from harmonic vibrational frequencies, obtained at the B3LYP/BSB level. This relatively high adsorption enthalpy suggests that Mg-functionalized R-Pyg[4]arenes can be envisaged as promising systems for molecular hydrogen storage.

© 2015 Elsevier B.V. All rights reserved.

1. Introduction

Molecular hydrogen is widely regarded as one of the most promising candidates to become the primary energy carrier for both industrial and mobile applications [1–3]. However, an economic model based on the use of hydrogen requires the implementation of very efficient methods for H₂ production, storage and use [4]. While production and use of hydrogen have been significantly

improved over the last few years [5–7], hydrogen storage has proved to be a more complicated problem [8]. Thus, it has been identified as the main obstacle in achieving the transition to the so-called Hydrogen Economy [9], which is intended to provide convenient solutions to: (i) environmental issues associated with the use of fossil fuels [10,11], (ii) the economic impact of the depletion of oil world reserves [12], and (iii) the high cost of oil extraction from non-conventional sources as tar-sands [13].

In order to understand the technological challenges involved in H₂ storage, it must be pointed out that molecular hydrogen, in its natural state, is a highly incompressible gas with low energy density [14]. Therefore, large amounts of hydrogen (i.e., large volumes) are necessary to produce a significant quantity of energy. In this

* Corresponding author at: Universidad San Francisco de Quito, Grupo de Química Computacional y Teórica (QCT-USFQ), Departamento de Ingeniería Química, Diego de Robles y Vía Interoceánica, Quito 17-1200-841, Ecuador.

E-mail address: jtorres@usfq.edu.ec (F.J. Torres).

regard, the U.S. Department of Energy has established that an adequate H₂ storage system must reach a content of 5.5 wt% until 2015 and 7.5 wt% until 2020 to completely replace fossil fuels in mobile applications [15,16].

Several methods have been proposed to address the problem of hydrogen storage [17]. The most common ones are high-pressure tanks and cryogenic containers; however, none of these methods have large-scale or mobile applications since their implementation involves extreme operating conditions (i.e., low temperature and high pressure) [17]. Alternative methods have been explored in the recent years, in particular, those involving physical absorption in microporous and other type of materials [18]. In the context of physisorption, the adsorbed hydrogen molecules retain their chemical nature while interacting with a host material through weak forces, that are the result of resonant fluctuations at the charge distribution (i.e., dynamical electron correlation) known as dispersive forces. This relatively weak interaction allows H₂ charge–discharge cycles to occur at moderate temperature and pressure conditions. The critical factor for the success of hydrogen physisorption as storage method resides in the characteristics of the material to be employed as media. In general terms, promising materials should possess a structure with either cavities or tunnels that are favorable for H₂ diffusion, adsorption, and release. Moreover, these materials should be composed of light elements in order to achieve significant H₂ content (wt%). As recently summarized by van den Berg and Otero-Aerán [19], in a very complete review on H₂ storage methods, different materials such as: carbon-based microporous solids [20–22], polymers with intrinsic microporosity (PIMs) [23,24], metal–organic frameworks (MOFs) [25–27], and zeolites [28–32] have been experimentally as well as theoretically evaluated as candidates for molecular hydrogen storage. For the case of microporous carbon-based materials, PIMs, and MOFs, it has been determined that their large surface area and microporous structure allow them to possess a reversible hydrogen storage capacity about ~7 wt% with corresponding adsorption enthalpy (ΔH_{ads}) values ranging from –6.8 to –8.2 kJ/mol [19]. Nonetheless, it must be pointed out that these notably high adsorption enthalpy values can be achieved only at liquid nitrogen temperature and a pressure of 20 bar because, as previously mentioned, the hydrogen interaction with these materials depends exclusively on the very weak dispersive forces. Stronger interactions have been determined for hydrogen molecules interacting with the polarizing centers (i.e., cations) of metal-functionalized materials [33,34] such as metal-exchanged zeolites [28–32,35–37]. A remarkably large ΔH_{ads} value of –17.5 kJ/mol has been reported for the particular case of magnesium-exchanged faujasite Y [38]. The latter experimentally determined value allows this material to be considered as an interesting candidate for hydrogen storage, taking into account that H₂ adsorption enthalpies significantly larger (in an absolute scale) than –15 kJ/mol are likely to be needed for operation near ambient temperature as proposed by Bhatia and Myers [39], as the result of a thorough thermodynamic analysis of the H₂ adsorption process in carbon materials. Although the latter is an important result, it must be indicated that Mg-exchanged faujasite Y has little potential as storage media for mobile applications, because its maximum H₂ uptake (i.e. <0.1 wt %) is far below the values suggested as optimal by the US Department of Energy.

In the present work, the potential of a class of macrocyclic compounds; namely R-substituted pyrogallol[4]arenes (R-Pyg[4]arenes; cavitands), as media for molecular hydrogen storage is theoretically evaluated by means of quantum–mechanical calculations. R-Pyg[4]arenes are versatile macromolecules that exhibit conformational control and adsorption selectivity [40] among other interesting properties. Of their known conformations, the cup-like *rccc* stereoisomer is of particular interest for the hydrogen

storage purpose, because it offers a wide enough cavity for trapping H₂ molecules [41] (see Fig. 1). Furthermore, as recently reported by Manzano et al. [42], a negative electrostatic potential is created inside the cavity of *rccc* R-Pyg[4]arenes by incorporating (during synthesis) electron-donating R groups at the lower rim of their structure. Because of the presence of this localized negative potential, positive ions can be embedded in the interior of the *rccc* R-Pyg[4]arenes giving rise to metal-functionalized species, whose polarizing centers could enhance the interaction with molecular hydrogen as observed in the case of metal-exchanged zeolites [28–32,35–37]. An additional advantage of metal-functionalized R-Pyg[4]arenes is the fact that these materials are composed mostly of light atoms (i.e., C, H, and O); therefore, they could adsorb higher H₂ amounts if compared with previously studied materials [20,21,23–32].

The present article is organized as follows: the construction of the models and the details of the adopted methods are summarized in Section 2; in Section 3, the results of the study are discussed, and finally the conclusions of this work are presented in Section 4.

2. Models and methods

As starting point for the construction of the metal-functionalized systems, we use the gas-phase molecular models of the *rccc* methyl- and 2-fluoro-ethyl-Pyg[4]arene (hereinafter referred to as fluoroethyl-Pyg[4]arene) reported elsewhere [42]. Four cations of different ionic size and charge; namely Li⁺, Na⁺, K⁺, and Mg²⁺, were added into the cavity of the two macrocyclic compounds to obtain the corresponding charged metal-functionalized species. As in the case of previously reported theoretical studies conducted to investigate the structural features of calix[4]arenes with alkali metal cations [43,44], negative counterions were not included in our metal-functionalized models, whose properties are expected to be mainly determined by cation– π interactions as suggested by Macias et al. [45]. All the gas-phase molecular models were visualized and modified by employing the program MOLDRAW [46]. The equilibrium position of the cations was determined by fully optimizing the models at the B3LYP/6-311G(d,p) level of theory as implemented in the Gaussian09 suit of programs [47]. Although *rccc* R-Pyg[4]arenes belong to the C₄ point group, no symmetry constraints were imposed during the optimization process with the objective of allowing the cations to move out of the principal symmetry axis. After optimization, subsequent vibrational calculations were used to confirm the located stationary points as true minima in the potential energy surface. Upon obtaining the optimal position of the different cations inside both methyl- and fluoroethyl-Pyg[4]arenes, a hydrogen molecule was added into the cavity of the different metal-functionalized systems to form a side-on (i.e., T-shaped) complex with the polarizing center. In all cases, a distance of 2 Å between the hydrogen center of masses and the cation was considered as the starting distance. Taking into consideration that the presence of the H₂ molecule is likely to have little effect on the structure of the macrocyclic compounds, only the cation and the hydrogen atoms were let free to move during the subsequent optimization stage carried out to obtain the equilibrium geometry for the H₂/M-R-Pyg[4]arene complexes. For the subsequent optimization process, the B3LYP functional was adopted as level of theory together with two basis sets of different flexibility; namely BSA: 6-311G(d,p) for all atoms and BSB: 6-311G(d,p) for M-R-Pyg[4]arene and a aug-cc-pVDZ for H₂. The use of the relatively larger basis functions is justified on the basis of the results reported by Torres et al. [35–37] who showed that the interaction between hydrogen's quadrupole and the polarizing centers of

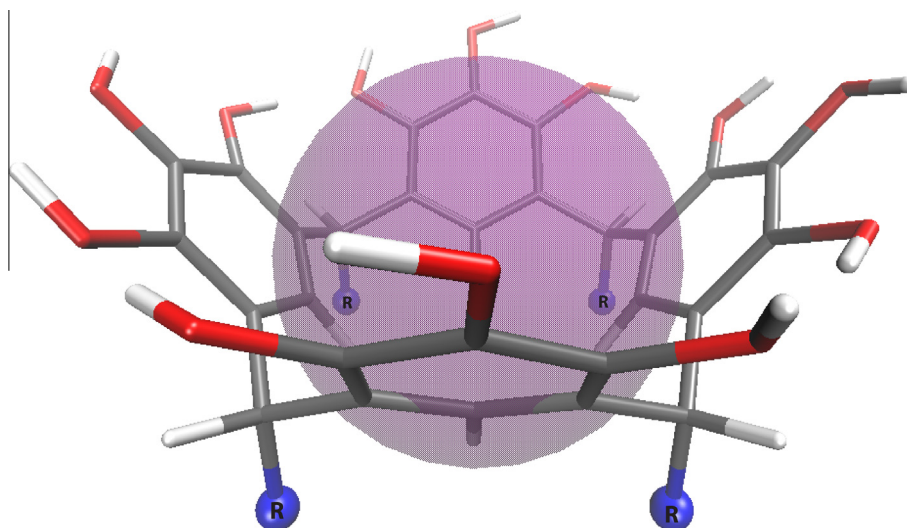


Fig. 1. Schematic representation of the cup-like conformation of R-substituted pyrogallol[4]arenes (i.e., rccc-R-Pyg[4]arenes) where the available space within its cavity is emphasized. For the sake of clarity, the R substituent groups, located at the lower rim of the macrocyclic molecule, are represented by blue spheres. Carbon, oxygen, and hydrogen atoms are represented with the gray, red, and white colors, respectively. (For interpretation of the references to color in this figure legend, the reader is referred to the web version of this article.)

metal-exchanged zeolites is more accurately described by adopting Dunning's correlation-consistent basis sets [48] for describing the adsorbed hydrogen molecule. On the equilibrium geometries of the different $H_2/M-R-Pyg[4]$ arene complexes, binding energies (BE) were computed by following the supermolecular approach:

$$BE = E_{Cav} + E_{H_2} - E_{H_2/Cav} \quad (1)$$

where E_{Cav} , E_{H_2} , and $E_{H_2/Cav}$ are computed electronic energies corresponding to the M-R-Pyg[4]arene macromolecule, the H_2 molecule, and the $H_2/M-R-Pyg[4]$ arene complex, respectively. Computed binding energies were further corrected for the basis set superposition error (BSSE) by employing the Boys–Bernardi counterpoise method [49]. Furthermore, the H_2 anharmonic stretching frequency was computed for all $H_2/M-R-Pyg[4]$ arene complexes on their corresponding equilibrium geometries at both B3LYP/BSA and B3LYP/BSB levels of theory in order to gain some insights on the dynamical behavior of the adsorbed H_2 molecule. The anharmonic vibrational stretching frequencies were computed by varying the position of the H atoms with respect of the molecule's center of masses at different points in the $-0.2/0.3 \text{ \AA}$ range (i.e., 26 points with a 0.02 \AA step). Then, a polynomial fit of sixth degree was used to obtain a potential energy function for which the one-dimensional Schrödinger equation was numerically solved by employing the scheme proposed by Lindberg [50]. The latter calculations were carried out by using our adopted version of the ANHARM module implemented in the CRYSTAL14 program [51,52] to compute the anharmonic stretching frequency of acidic Brønsted sites in crystalline materials [53,54]. For further details of the ANHARM's scheme the reader is referred to Ref. [54].

It is well known that traditional DFT methods, including those based on hybrid functionals such as B3LYP, fail in describing the weak dispersive forces [55], which in turn, have been shown to be relevant in the computational description of the hydrogen adsorption on the polarizing centers of microporous materials [37]. In an effort to include the dispersive forces in the description of the different complexes considered in the present study, two different approaches were adopted: (i) the functional B97D was employed instead of the functional B3LYP for describing the H_2 adsorption [56–59], and (ii) the B3LYP results were refined by employing MP2 calculations within the frame of the ONIOM approach [60]. The purpose of adopting two different approaches

is to evaluate the performance of each scheme and determine which one of them provides reliable estimates of the binding energy for the various $H_2/M-R-Pyg[4]$ arene complexes at a moderate computational cost.

For details on the theoretical aspects of the dispersion-corrected B97D functional (i.e., a GGA-type functional) the reader is referred to Refs. [56–59], here it is noteworthy to recall that the functional B97D contains a Grimme's pair-wise empirical corrective term for including *a posteriori* dispersive forces in a DFT calculation according to:

$$E_{DFT-D} = E_{KS-DFT} + E_{Disp} \quad (2)$$

where E_{KS-DFT} is the system energy obtained by solving self-consistently the Kohn–Sham equations upon the selection of a certain exchange–correlation functional, and E_{Disp} is the energy term associated with the forces of dispersion that are estimated by means of the following expression:

$$E_{Disp} = -s_6 \sum_{i=1}^{N_{at}-1} \sum_{j=i+1}^{N_{at}} \frac{C_6^{ij}}{R_{ij}^6} f_{dmp}(R_{ij}) \quad (3)$$

in the latter expression, N_{at} is the number of atoms in the system, C_6^{ij} denotes the dispersion coefficient that is computed as a geometric mean (i.e., $C_6^{ij} = (C_6^i C_6^j)^{1/2}$) for the pair of atoms ij , s_6 is a global scaling factor that depends exclusively on the exchange–correlation functional employed to calculate E_{KS-DFT} , and R_{ij} is the distance between the i -th and the j -th atoms. Within the Grimme's scheme, a distance damping function f_{dmp} is used to include the correction only at relevant distances. The f_{dmp} function is given by:

$$f_{dmp}(R_{ij}) = \frac{1}{1 + e^{-d(R_{ij}/R_r - 1)}} \quad (4)$$

where R_r is the sum of the van der Waals radius R_{vdW} of the i -th and the j -th atoms and d is a damping factor. In the present work, Grimme's default values as included in Gaussian 09 for s_6 , C_6^i , R_{vdW} , and d have been used for all the calculations.

As aforementioned, an ONIOM scheme [60] was also employed in the present work for the theoretical description of the H_2 adsorption in M-R-Pyg[4]arenes. This approach consists in the division of the complex in two layers referred to as *real* and *model*

systems. The real system is the whole H₂/M-R-Pyg[4]arene complex, which is described at a low level of theory, whereas the model system contains only the portion of the complex that is relevant to the H₂ interaction (i.e., the H₂ molecule, the polarizing center, and some atoms of their neighborhood) and is described at both the low and the high levels of theory. Within the frame of the ONIOM approach, the binding energies are computed with the following expression:

$$BE_{\text{ONIOM}}^{\text{C}} = BE_{[\text{LOW:REAL}]}^{\text{C}} + \left(BE_{[\text{HIGH:MODEL}]}^{\text{C}} - BE_{[\text{LOW:MODEL}]}^{\text{C}} \right) \quad (5)$$

where $BE_{[\text{LOW:REAL}]}^{\text{C}}$ is the BSSE-corrected binding energy computed at the low level for the real system, and $BE_{[\text{HIGH:MODEL}]}^{\text{C}}$ and $BE_{[\text{LOW:MODEL}]}^{\text{C}}$ are the BSSE-corrected binding energies computed in the model system at the high and low levels of theory, respectively.

Because quantum-mechanical methods based on the wavefunction expansion are required to describe the dynamical electron correlation, which in turn is the origin of the dispersive forces, the Møller-Plesset perturbation method truncated at the second order (MP2) [61,62] was adopted as the high level of theory together with both BSA and BSB. It must be pointed out that this scheme assumes that intra- and intermolecular interactions for the B3LYP and MP2 methods (low and high levels, respectively) cancel out at the model layer, so that the remaining fraction can be attributed entirely to the forces of dispersion.

3. Results and discussion

For a sake of clarity, this section is divided into three parts: first, we discuss the geometrical features of the M-R-Pyg[4]arenes to analyze the effect of the charge and the size of the cations (i.e., Li⁺, Na⁺, K⁺, and Mg²⁺) on the structure of the system. Next, we discuss the B3LYP/6-311G(d,p) results concerning the adsorption of H₂ on M-R-Pyg[4]arenes with particular emphasis made in the computed binding energy and the activation of the H₂ due to the interaction with the cations explained on the basis of computed H–H anharmonic frequency red-shifts. Finally, we discuss the inclusion of the forces of dispersion in the description of the systems by employing both the B97D functional and the MP2 method as high level in the ONIOM scheme.

3.1. Geometrical description of M-R-Pyg[4]arenes

Table 1 presents the geometrical features of the optimized metal-functionalized R-Pyg[4]arenes calculated at the B3LYP/6-311G(d,p) level of theory.¹ In particular, the second column of Table 1 shows the values of the distance between the metal cation and the *i*-th (*i* = 1–8) carbon atom belonging to the lower rim of the R-Pyg[4]arenes, which are labeled as illustrated in Fig. 2. In the case of the monovalent cations, it is observed that their distances with respect to the lower rim atoms increase with respect to the size of the cation: Li⁺ < Na⁺ < K⁺, while for Mg²⁺ the distance is always shorter than for Li⁺. Taking into account that for the metal-free macromolecules, the atoms C₁, C₃, C₅, and C₇, as well as, C₂, C₄, C₆, and C₈ are related by symmetry (i.e., R-Pyg[4]arenes belong to the C₄ point group), the $D_{\text{M-C}_i}$ distances reported in Table 1 indicate that for both, the methyl and the fluoroethyl derivatives, the Na⁺ and K⁺ cations are located at the center of the lower rim. In contrast, the smaller Li⁺ cation slightly deviates from this position. It is important to point out that, due to the very symmetric structure of metal-free R-Pyg[4]arenes, additional stable positions (i.e., minima of the potential energy surface) for the small Li⁺ ion are expected to exist

Table 1

Geometrical features of the metal-functionalized R-Pyg[4]arenes optimized at the B3LYP/6-311G(d,p) level of theory. $D_{\text{M-C}_i}$ is the distance between the cation and the *i*-th carbon atom of the R-Pyg[4]arene lower rim (labels in Fig. 2). $D_{\text{M-Bcup}}$ is the distance between the cation and the center of mass of the lower rim of the different R-Pyg[4]arenes. The charge of the embedded q_{M} cations and the BSSE-corrected binding energy BE^{C} are also reported. Distances, angles, charges and energies are in Å, degrees, e, and kJ/mol respectively. The equilibrium geometries of all the M-R-Pyg[4]arenes are available as [Supplementary Information](#).

	$D_{\text{M-C}_i}$ (<i>i</i> = 1, 2, 3, 4, 5, 6, 7, 8)								$D_{\text{M-Bcup}}$	q_{M}	BE^{C}
<i>R</i> = methyl											
Mg	3.66	2.54	3.66	2.54	3.66	2.54	3.66	2.54	0.589	0.956	967.5
Li	3.64	2.62	3.71	2.71	3.77	2.71	3.70	2.62	0.823	0.660	250.9
Na	3.80	2.81	3.80	2.81	3.80	2.81	3.80	2.81	1.150	0.708	209.5
K	4.06	3.15	4.06	3.15	4.06	3.15	4.06	3.15	1.878	0.821	161.1
<i>R</i> = fluoroethyl											
Mg	3.66	2.54	3.66	2.54	3.67	2.54	3.66	2.54	0.581	0.957	919.8
Li	3.59	2.58	3.72	2.76	3.83	2.74	3.70	2.57	0.813	0.652	224.9
Na	3.80	2.80	3.80	2.80	3.80	2.80	3.80	2.80	1.162	0.694	184.0
K	4.07	3.16	4.07	3.16	4.07	3.16	4.07	3.16	1.891	0.808	135.6

within the cavity of the macrocyclic compound. Nonetheless, only the one obtained during the optimization process is considered for the further analysis of the interaction with molecular hydrogen. Although the ionic radius of Mg²⁺ is very close to that of Li⁺, the magnesium atom is also located at a central position, and it is embedded deeper in the cavity of the macrocyclic molecules. The third column of Table 1 shows the distance between the center of mass of the lower rim of the macrocyclic molecule and the metal cation (i.e., depth of the cation inside the cavity). This distance follows the Mg²⁺ < Li⁺ < Na⁺ < K⁺ trend for both methyl- and fluoroethyl-substituted derivatives. Interestingly, it is observed that the presence of a negative electrostatic potential expected in the interior of the methyl-Pyg[4]arene, as proposed in Ref. [42], has a negligible effect on the position of the embedded cations since the resulting $D_{\text{M-Bcup}}$ distances for each metal are about the same in both the methyl- and the fluoroethyl-substituted systems. It is also important to indicate that the presence of metallic ions has a negligible effect on the structure of the different R-Pyg[4]arenes since insignificant changes were observed when comparing the free-metal macrocyclic compounds with the various metal-functionalized systems. Concerning the electronic character of the systems under investigation, the last column of Table 1 reports the Mulliken charge of the metal cations embedded in the different R-Pyg[4]arenes. As expected, the divalent cation Mg²⁺ possesses a larger charge than the monovalent cations. In agreement with the resulting $D_{\text{M-Bcup}}$ distances, the charge of the monovalent cations follows the trend: K⁺ > Na⁺ > Li⁺, which indicates that the shorter the distance between the cation and the lower rim of the R-Pyg[4]arene the higher the effect of the chemical environment over the embedded metal. The same conclusion applies for the magnesium cation, whose charge decreases to half (i.e., from 2+ to 0.956+) since it is the closest cation to the base of the macrocyclic compounds for the two substituted derivatives.

In summary, results of Table 1 show that the position of metal cations inside the cavity of R-Pyg[4]arenes is almost independent of the R substituent group, but the distance $D_{\text{M-Bcup}}$ in turn depends on the ionic radius, polarizing character, and charge, being all these characteristics exclusively associated to the metallic species. Although the latter observation is noteworthy, it is expected that cations embedded in the cavity of methyl-Pyg[4]arene compound are subject of a greater binding force compared with the fluoroethyl-substituted system as determined by Manzano et al. for the case of a NH₄⁺ ion interacting with Pyrogallol[4]arenes with various R-substituent groups [42]. The latter statement is confirmed by the BSSE-corrected binding energies (BE^{C}) computed for the different M-R-Pyg[4]arene systems and reported in the last column of Table 1, where it is observed that the values obtained for the methyl derivatives are consistently larger than those obtained

¹ The equilibrium geometries of all the M-R-Pyg[4]arenes are available as [Supplementary Information](#).

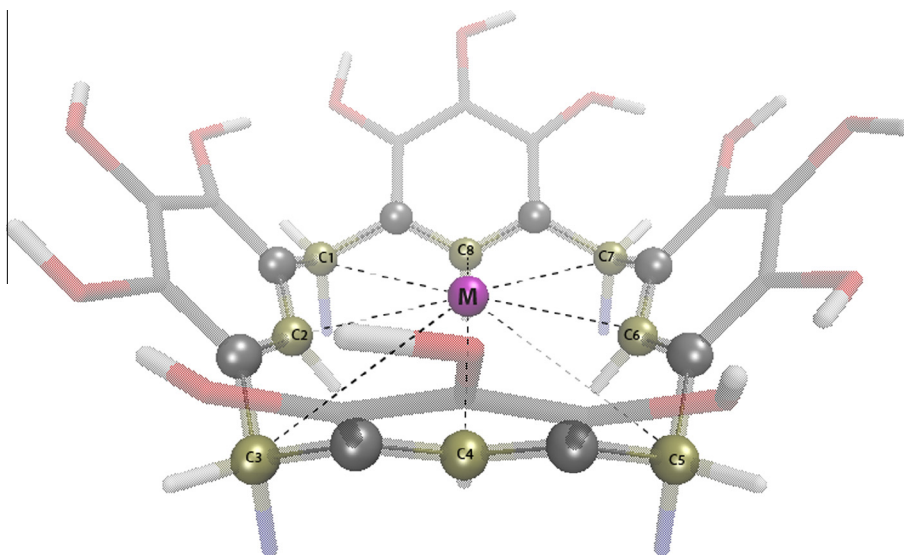


Fig. 2. Local environment of a cation embedded in the cavity of a *rccc* R-Pyg[4]arene. The distances between each one of the carbon atoms that belong to the lower rim of the macrocyclic molecule (i.e., C1–C8) and the cation are summarized in Table 2 for all the metal-functionalized systems investigated in the present work. Carbon, oxygen, and hydrogen atoms are represented with the gray, red, and white colors, respectively. The magenta sphere represents the embedded cation. (For interpretation of the references to color in this figure legend, the reader is referred to the web version of this article.)

for their fluoroethyl-substituted counterparts. It is important to point out that the great BE^c values of Table 1 are in good agreement with previously reported studies on cations interacting with calix [4]arenes [45].

3.2. H_2 interaction with M-R-Pyg[4]arenes

Table 2 summarizes the results regarding the binding energy computed for the different H_2 /M-R-Pyg[4]arene complexes as well as their relevant geometry features as obtained by employing the B3LYP functional together with the two different basis sets considered in this work.² Data reported in Table 2 shows that for both, methyl- and fluoroethyl-substituted derivatives, the distance between the H_2 center of mass and the metal cation (D_{M-H_2}) increases in the order $Li^+ < Mg^{2+} < Na^+ < K^+$. This trend is observed in the results obtained with the two basis sets; however, the D_{M-H_2} distances obtained with BSB are consistently shorter than the values computed with BSA. The reduction is more significant (i.e., ~3%) in the case of the K-functionalized derivatives, which indicates that the polarizing effect of the K^+ cation on the H_2 molecule is remarkably enhanced when the adsorbed molecule is described with the aug-cc-pVDZ basis set. Nevertheless, some influence of Basis-Set Superposition Error (BSSE) is also expected in the results obtained at the B3LYP/BSB level of theory, as we will discuss later on in the present section.

From Table 2, it is also evident that the H_2 /Mg-R-Pyg[4] arene (R = methyl and fluoroethyl) complexes present the largest increment in the adsorbed H_2 interatomic distance (ΔD_{H-H}), being equal to +1.1% and +0.7% with respect to the interatomic distance of the isolated gas-phase hydrogen molecule described at the B3LYP/BSA and B3LYP/BSB levels, respectively. For the systems containing monovalent cations, the ΔD_{H-H} value obtained at the B3LYP/BSA level increases in the order $K^+ < Na^+ < Li^+$ for both methyl- and fluoroethyl-substituted derivatives. However, the ΔD_{H-H} changes obtained at the B3LYP/BSB level are about the same for all complexes (i.e., ~0.0015 Å) independently on the nature of the monovalent cation or the R-substituent group of the macrocyclic molecule. In agreement with the previous results, the red-shift of

the anharmonic H–H stretching frequency ($\Delta \bar{\nu}_{H-H}$) obtained for the H_2 /Mg-R-Pyg[4]arene complexes is significantly larger than the values obtained for the Li, Na, and K-functionalized systems, showing that the Mg^{2+} ion embedded in R-Pyg[4]arenes possesses a greater capability to activate the H–H bond in comparison to the monovalent cations embedded within the same systems. The $\Delta \bar{\nu}_{H-H}$ values computed for the H_2 /Mg-methyl-Pyg[4] arene complex are -124.2 cm^{-1} and -104.3 cm^{-1} for BSA and BSB, respectively; whereas, for the case of the H_2 /Mg-fluoroethyl-Pyg[4] arene complex slightly larger values were obtained (i.e., -149.0 cm^{-1} and -137.5 cm^{-1}). It is worth mentioning that such a notable change in the anharmonic H–H stretching frequency is in reasonable agreement with a previous experimental study on the H_2 interacting with magnesium-exchanged faujasite Y, where a $\Delta \bar{\nu}_{H-H}$ value of -107 cm^{-1} was determined by means of FTIR spectroscopy experiments conducted at the temperature range 121–146 K [38]. For the case of R-Pyg[4]arenes functionalized with monovalent cations, $\Delta \bar{\nu}_{H-H}$ values computed at the B3LYP/BSA level of theory span the -20 cm^{-1} to -65 cm^{-1} range and follow the trend: $Li^+ > Na^+ > K^+$; whereas, the values obtained at the B3LYP/BSB level of theory span the slightly narrower -42 cm^{-1} to -63 cm^{-1} range and follow the trend: $Li^+ \sim Na^+ > K^+$. It must be indicated that the trend in the $\Delta \bar{\nu}_{H-H}$ values obtained in our calculations for the Na-functionalized systems are also in good agreement with experimental observations (i.e., -39 cm^{-1} and -46 cm^{-1}) [38].

As a direct consequence of the great capability of the Mg^{2+} ion to activate the adsorbed H_2 molecule, remarkably large BSSE-uncorrected binding energies (BE columns in Table 2) of about $\sim 17.0 \text{ kJ/mol}$ and $\sim 24.0 \text{ kJ/mol}$ are obtained at the B3LYP/BSA and B3LYP/BSB levels, respectively, for the different H_2 /Mg-R-Pyg[4] arene complexes. The increment of about $\sim 7 \text{ kJ/mol}$ in the computed BE of the H_2 /Mg-R-Pyg[4] arene complexes when going from BSA to BSB is consistent with our previous theoretical studies [35–37], and it is also observed in the case of the systems containing monovalent cations for which computed BE take values between 2.8 kJ/mol and 11.3 kJ/mol for BSA and between 9.0 kJ/mol and 18.6 kJ/mol for BSB, being the largest BE values in the latter ranges associated to the different H_2 /Li-R-Pyg[4] arene complexes (see Table 2). Upon correction for the Basis Set Superposition Error (BSSE), a decrement in the binding energy values is observed in

² The equilibrium geometries of all the H_2 /M-R-Pyg[4]arenes are available as Supplementary Information.

Table 2
Geometrical features, BSSE-uncorrected (BE), and BSSE-corrected (BE^c) binding energies of the H₂/M-R-Pyg[4]arene complexes optimized at the B3LYP/BSA and B3LYP/BSB levels of theory. D_{M-H_2} is the distance between the center of mass of the H₂ molecule and the cation and ΔD_{H-H} is the change in the H–H interatomic distance of the adsorbed molecule as compared with the value obtained for an isolated H₂ molecule. The change in the anharmonic H–H stretching frequency ($\Delta\bar{\nu}_{H-H}$) is also reported. Distances, frequencies and energies are in Å, cm⁻¹, and kJ/mol, respectively. The equilibrium geometries of all the H₂/M-R-Pyg[4]arenes are available as [Supplementary Information](#).

	B3LYP/BSA					B3LYP/BSB				
	D_{M-H_2}	ΔD_{H-H}^a	BE	BE ^c	$\Delta\bar{\nu}_{H-H}^b$	D_{M-H_2}	ΔD_{H-H}^a	BE	BE ^c	$\Delta\bar{\nu}_{H-H}^b$
<i>R = methyl</i>										
Mg	2.2277	0.0085	16.7	14.2	-124.2	2.1993	0.0050	24.5	17.0	-104.3
Li	2.0613	0.0042	10.8	8.8	-63.7	2.0219	0.0012	17.9	11.0	-51.3
Na	2.4862	0.0025	5.8	4.3	-49.2	2.4663	0.0016	13.6	5.6	-62.9
K	3.1269	0.0012	2.8	2.1	-20.2	3.0001	0.0014	9.0	2.3	-44.8
<i>R = fluoroethyl</i>										
Mg	2.2334	0.0083	15.9	13.3	-149.0	2.2095	0.0050	23.4	15.7	-137.5
Li	2.0579	0.0043	11.3	8.8	-64.8	2.0147	0.0013	18.6	10.9	-58.6
Na	2.4950	0.0024	5.7	4.2	-39.3	2.4632	0.0015	13.8	5.5	-60.9
K	3.1133	0.0013	3.0	2.1	-20.9	3.0142	0.0012	10.0	2.3	-42.1

^a D_{H-H}^{ref} : 0.74425937 Å and 0.76086464 Å for B3LYP/BSA and B3LYP/BSB levels of theory, respectively.

^b $\bar{\nu}_{H-H}^{ref}$: 4195.7 cm⁻¹ and 4141.5 cm⁻¹ for B3LYP/BSA and B3LYP/BSB levels of theory, respectively.

all the studied complexes. As reported in [Table 2](#), a difference of -2.5 kJ/mol is found when comparing BE and BE^c values obtained at the B3LYP/BSA level for the H₂/Li-R-Pyg[4] arene and H₂/Mg-R-Pyg[4]arene complexes. On the other hand, the BE^c – BE difference is less significant in the case of Na- and K-functionalized complexes which were computed to be -1.5 kJ/mol and -0.7 kJ/mol, respectively. As expected, the BSSE effect is particularly dramatic in the case of the results obtained at the B3LYP/BSB level of theory due to the intrinsic limitations of the 6-311G(d,p) basis sets in describing the embedded cations, which in turn take advantage of the larger aug-cc-pVDZ basis set employed to describe the adsorbed H₂ molecule. For all the complexes under investigation, the BE^c – BE difference obtained with BSB is approximately -7.7 kJ/mol, representing a decrease of about ~75% for the particular case of H₂/K-R-Pyg[4]arenes complexes (see [Table 2](#)). Comparison of the BE^c values, obtained with the different basis sets for all the complexes, show that BSSE-corrected values computed with BSB are always larger than the corresponding BSA values. In the specific case of the H₂/Mg-R-Pyg[4]arene complexes, an increment of 2.4 kJ/mol was computed when R = fluoroethyl, whereas an increment of 2.8 kJ/mol was obtained for the system with R = methyl. The extra stabilization of the complexes associated to the previous values can be entirely attributed to a better description of the M⁺-H₂ interaction (i.e., ion–quadruple interaction) achieved when flexible enough basis sets are adopted for describing the hydrogen molecule in adsorptive processes.

3.3. Inclusion of the forces of dispersion

[Table 3](#) summarizes calculated BSSE uncorrected and corrected binding energies (BE and BE^c, respectively) for the different H₂/M-R-Pyg[4]arene complexes calculated with the B97D functional together with both BSA and BSB basis sets. In conformity with the results obtained with the B3LYP functional, data reported in [Table 3](#) shows that the binding energy values computed with BSB are consistently larger than the results obtained with BSA for all the complexes under investigation. The aforementioned increment is notably large when observing the BSSE-uncorrected B97D binding energies, being as large as one order of magnitude in the particular case of the K-functionalized complexes. More moderate increments are appreciated when comparing BSSE-corrected B97D binding energies. Besides this preliminary observation, comparison between the data reported in [Table 3](#) and results included in [Table 2](#) shows that BE^c values obtained at the B97D level are as expected substantially larger than their corresponding

Table 3

BSSE-uncorrected (BE) and BSSE-corrected (BE^c) binding energies computed for the different H₂/M-R-Pyg[4]arene complexes employing the B97D functional and the ONIOM scheme with both BSA and BSB basis sets. Energies are in kJ/mol.

	BE _{B97D}		BE ^c _{B97D}		BE _{ONIOM}		BE ^c _{ONIOM}	
	BSA	BSB	BSA	BSB	BSA	BSB	BSA	BSB
<i>R = Methyl</i>								
Mg	28.6	35.2	26.8	27.8	24.7	34.3	19.2	22.0
Li	30.5	38.3	28.9	30.9	15.4	22.8	10.1	10.8
Na	21.1	29.5	19.6	20.9	7.9	10.9	4.6	5.8
K	9.2	19.8	8.3	11.0	4.5	6.7	2.7	3.0
<i>R = Fluoroethyl</i>								
Mg	29.1	35.7	27.3	28.1	25.5	34.0	20.0	23.6
Li	30.7	38.5	28.9	30.7	17.6	26.6	12.1	14.1
Na	21.0	30.1	19.4	21.1	8.6	11.4	5.3	6.8
K	9.2	19.9	8.2	11.3	5.5	8.6	3.7	4.8

B3LYP results. In the particular cases of the H₂/Na-R-Pyg[4]arene and H₂/Li-R-Pyg[4]arene complexes, the BE^c_{B97D} – BE^c_{B3LYP} difference is ~15 kJ/mol and ~20 kJ/mol for both BSA and BSB respectively, indicating that the B97D functional seems to significantly overestimate the contribution of the dispersive forces in the description of non-bonded complexes involving metallic ions. The latter statement is supported by the recent results of Kocman et al. who have determined that formation energy estimates of the H₂-Li-functionalized-coronene adduct are overestimated at the B97D level upon comparison with CCSD(T)/CBS and quantum Monte Carlo calculations [63]. Thus, it is rather important to state that, although the use of the B97D functional is advantageous from the point of view of computational costs (i.e., B97D computational times are within the typical range of other standard DFT functionals), this functional leads to unrealistic too large binding energies and is then not completely adequate for describing the H₂ adsorption on the polarizing centers of M-R-Pyg[4]arenes.

[Table 3](#) also summarizes the BSSE-uncorrected and BSSE-corrected binding energies computed at the MP2 level. As mentioned before in the Models and Methods section, the MP2 calculations were carried out within the frame of the ONIOM approach with the sole purpose of evading excessive computational efforts; however, it must be acknowledged that this scheme represents an additional effort in comparison to the B97D level since a number calculations must be performed due to the subdivision of the complex in the real and model layers. The portion of the H₂/M-R-Pyg[4]arene complexes adopted as model system is shown in [Fig. 3](#) where it can be observed that special attention was made in cutting out a model as regular as possible. The latter

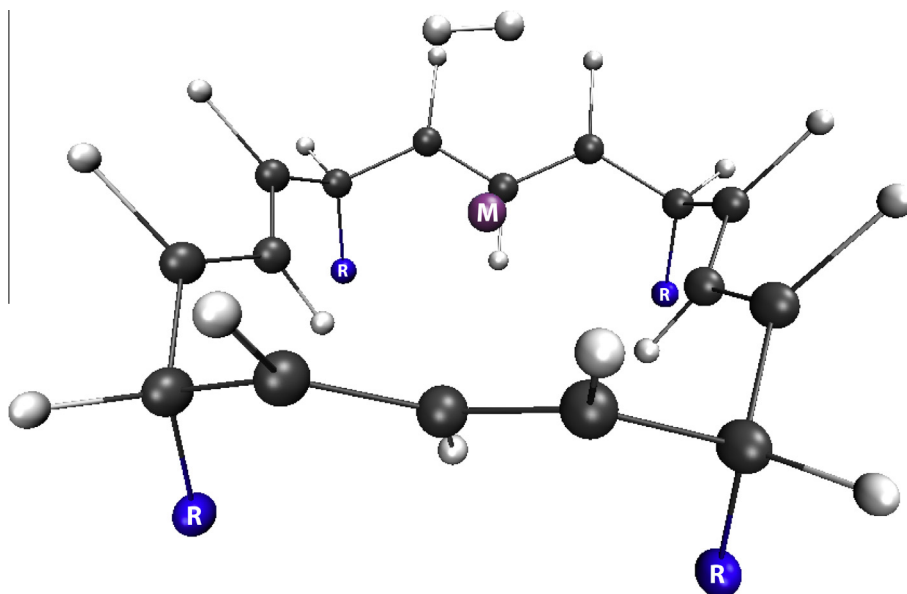


Fig. 3. Portion of atoms of the $H_2/M-R$ -Pyg[4]arene complexes employed as model system in the ONIOM calculations of the present work. Dangling bonds were saturated by adding hydrogen atoms. For the sake of clarity, the R substituent groups located at the lower rim of the macrocyclic molecule are represented by blue spheres. Carbon and hydrogen atoms are represented with the gray and white colors, respectively. The magenta sphere represents the embedded cation. (For interpretation of the references to color in this figure legend, the reader is referred to the web version of this article.)

consideration is justified since unbalanced or extremely non-symmetrical models could lead to the presence of artificial electric dipoles (or even higher-degree moments), which in turn, might cause overestimated results as previously reported by some of the authors of the present work [35]. Inspection of the ONIOM data shows that for this method strong basis set size effects are also present, representing increments in the 2.2–9.6 kJ/mol range for BSSE-uncorrected binding energies and in the 0.3–3.6 kJ/mol range for BSSE-corrected values. In contrast with the B97D results, the largest increments of the latter ranges were observed for the $H_2/Mg-R$ -Pyg[4]arene complexes. From the last columns of Table 3, it is observed that the largest BE_{ONIOM}^c and BE_{ONIOM}^s energy values are also obtained for the $H_2/Mg-R$ -Pyg[4]arene complexes and, for systems with monovalent cations, decreases in the following order: $Li^+ > Na^+ > K^+$, which is consistent with the trend observed in the case of B3LYP results. The $BE_{ONIOM}^c - BE_{B3LYP}^c$ differences, associated with the inclusion of the dispersive forces in the description of the different complexes, are moderate in the case of the Li-, Na-, and K-functionalized systems, belonging to the 0.5–3.3 kJ/mol range. Nonetheless, for the $H_2/Mg-R$ -Pyg[4]arene complexes, the $BE_{ONIOM}^c - BE_{B3LYP}^c$ difference reach values as large as 8 kJ/mol for R = fluoroethyl. This result is in reasonable agreement with previous studies where a similar ONIOM approach was adopted to study the $Mg^{2+}-H_2$ adduct embedded in a zeolite periodic framework [35]. Moreover, it gives rise to a BE_{ONIOM}^c value of 23.6 kJ/mol, which, to the authors' best knowledge, is among the largest interaction energy ever determined for any material by means of quantum-mechanical approaches [19,63].

In order to assess, at least from a theoretical point of view, the potential applicability of R-M-Pyg[4]arenes as media for molecular hydrogen storage, the zero point energy correction and the thermal corrections at 298 K were obtained for the H_2/Mg -fluoroethyl-Pyg[4]arene complex, using the harmonic vibrational frequencies computed at the B3LYP/BSB level and the standard expressions for an ideal gas in the canonical ensemble. By adding these corrections to the BE_{ONIOM}^c (BSB values) of Table 3, a ΔH_{ads}^0 value of -17.6 kJ/mol is estimated for the H_2 adsorption process on the polarizing center of Mg-exchanged fluoroethyl-Pyg[4]arene. The latter enthalpy of adsorption is above the value proposed by Bhatia and

Myers [39] as optimal for storage operation near ambient temperature, and it is close to the experimentally determined value for (Na,Mg)-exchanged Y zeolite reported by Turnes-Palomino et al. [38], with the additional advantage implicit in the fact that R-Pyg[4]arenes are lighter chemical matrices than zeolites. The results here reported allow Mg-functionalized R-Pyg[4]arenes to be proposed as potentially applicable system for H_2 capture, and they could be envisaged as basic elements in the future development of materials for hydrogen storage by means of physisorption.

4. Conclusions

In the present work we have investigated the potential of various metal-functionalized R-substituted pyrogallol[4]arenes as media for molecular hydrogen storage within the framework of quantum-mechanical theoretical calculations. The various species evaluated in the present study were constructed by considering $M = Li^+, K^+, Na^+, Mg^{2+}$ and $R = \text{methyl and fluoroethyl}$. As the first step of the study, we have determined the equilibrium structure of the different M-R-Pyg[4]arenes compounds by means of a full optimization process without imposing symmetric constrains. As a result of the first stage, it was observed that the position of the metal ions inside the cavity of the macrocyclic compounds is independent of the electron-donating/electron-withdrawing character of the R substituent group, but the location of these ions was found to depend on the ionic radius, the polarizing character, and the charge of each cation. In general terms, it was observed that Mg^{2+} and Li^+ are embedded deeper in the cavity of the R-Pyg[4]arenes in comparison with the bulkier Na^+ and K^+ ions. As a direct result of the latter, significant changes were determined on the computed Mulliken charges of magnesium and lithium atoms, whose charge notably decreases when embedded in both methyl- and fluoroethyl-Pyg[4]arenes.

As a second step of the study, we focused our attention on the determination of the binding energies arising from the interaction between a hydrogen molecule added close to the cation of the different M-R-Pyg[4]arenes previously optimized. BSSE-corrected binding energies (BE^c) obtained at the B3LYP level were observed to follow the trend $K^+ < Na^+ < Li^+ < Mg^{2+}$. Moreover, an increment

of about ~ 3 kJ/mol was obtained for the BE^c values when going from BSA to BSB, which gives rise to the significantly larger values of 15.7 kJ/mol and 17.0 kJ/mol computed for the H_2/Mg -fluoroethyl-Pyg[4]arene and H_2/Mg -methyl-Pyg[4]arene complexes, respectively. Following the aforementioned tendency, substantial changes in the H–H anharmonic stretching frequency were determined for the complexes containing the Mg^{2+} ion, being the computed $\Delta\bar{\nu}_{H-H}$ as large as -137.5 cm^{-1} , which is in good agreement with values experimentally determined by means of FTIR, conducted on the H_2/Mg -exchanged faujasite Y. Two different methods; namely: (i) the B97D functional and (ii) the MP2 method within the framework of the ONIOM approach, were tested to include the contribution of dispersive forces in the description of the different $H_2/M-R$ -Pyg[4]arene complexes. Results reported in the present work, allow us to conclude that the B97D functional seems to overestimate the contribution of dispersive forces for the $H_2/M-R$ -Pyg[4]arene complexes since too large increments were observed when comparing the BE_{B97D}^c values with their corresponding values computed with the B3LYP functional. The latter statement applies particularly to the Li- and Na-functionalized systems (i.e., up to 20.1 kJ/mol and 15.2 kJ/mol computed as the $BE_{B97D}^c - BE_{B3LYP}^c$ difference, respectively), and it is supported by a recently reported theoretical study on the interaction of H_2 with the polarizing centers of coronene model systems containing Li^+ ions. On the other hand, BE^c values obtained at the MP2 level by adopting the ONIOM approach resulted in more moderate increments upon comparison with the corresponding B3LYP values. The largest increment was obtained for the H_2/Mg -fluoroethyl-Pyg[4]arene complex, and it was computed to be about ~ 8 kJ/mol (i.e., $BE_{MP2}^c - BE_{B3LYP}^c$ difference), being this increment consistent with results previously reported by some of the authors of the present work. Finally, a remarkably large adsorption enthalpy value, $\Delta H_{ads}^0 = -17.6$ kJ/mol, was estimated for the H_2/Mg -fluoroethyl-Pyg[4]arene complex by adding the zero point energy and thermal corrections at 300 K to the resulting BE_{MP2}^c value. This relatively high adsorption enthalpy value implies that the Mg-functionalized R-Pyg[4]arenes can be considered as a key element for the design of materials for molecular hydrogen storage.

Acknowledgements

This study has been performed by employing the computational resources of USFQ's High Performance Computing System (HPC-USFQ). The authors would like to thank USFQ's Collaboration Grants program and UBx's Initiative d'Excellence (IdEx) for financial support. FJT thanks Prof. Piero Ugliengo from Università degli Studi di Torino for sharing fundamental ideas regarding the ANHARM code.

Appendix A. Supplementary material

Supplementary data associated with this article can be found, in the online version, at <http://dx.doi.org/10.1016/j.comptc.2015.08.017>.

References

- [1] N.V.S.N.M. Konda, N. Shah, N. Brandon, Dutch hydrogen economy: evolution of optimal supply infrastructure and evaluation of key influencing elements, *Asia-Pac. J. Chem. Eng.* 7 (2012) 534–546.
- [2] A.I. Miller, R.B. Duffey, Sustainable supply of global energy needs and greenhouse gas reductions, *Trans. Can. Soc. Mech. Eng.* 33 (2009) 1–9.
- [3] A. Zuetel, A. Remhof, A. Borgschulte, O. Friedrichs, Hydrogen: the future energy carrier, *Philos. T. Roy. Soc. A* 368 (2010) 3329–3342.
- [4] S. Dunn, Hydrogen futures: toward a sustainable energy system, *Int. J. Hydrogen Energy* 27 (2002) 235–264.
- [5] A. Bulut, M. Yurderi, Y. Karatas, M. Zahmakiran, H. Kivrak, M. Gulcan, M. Kaya, Pd-MnOx nanoparticles dispersed on amine-grafted silica: highly efficient

- nanocatalyst for hydrogen production from additive-free dehydrogenation of formic acid under mild conditions, *Appl. Catal. B-Environ.* 164 (2015) 324–333.
- [6] A. Hassan, V.A. Paganin, E.A. Ticianelli, Pt modified tungsten carbide as anode electrocatalyst for hydrogen oxidation in proton exchange membrane fuel cell: CO tolerance and stability, *Appl. Catal. B-Environ.* 165 (2015) 611–619.
- [7] P. Parthasarathy, K.N. Sheeba, Combined slow pyrolysis and steam gasification of biomass for hydrogen generation—a review, *Int. J. Energy Res.* 39 (2015) 147–164.
- [8] A.J. Churchard, E. Banach, A. Borgschulte, R. Caputo, J.-C. Chen, D.C. Clary, K.J. Fijalkowski, H. Geerlings, R.V. Genova, W. Grochala, T. Jaron, J.C. Juanes-Marcos, B. Kasemo, G.-J. Kroes, I. Ljubic, N. Naujoks, J.K. Norskov, R.A. Olsen, F. Pendolino, A. Remhof, L. Romaszki, A. Tekin, T. Vegge, M. Zach, A. Zuetel, A multifaceted approach to hydrogen storage, *Phys. Chem. Chem. Phys.* 13 (2011) 16955–16972.
- [9] U. Bossel, B. Eliasson, Energy and the Hydrogen Economy, ABB Switzerland Ltd., Corporate Research, Switzerland, 2006.
- [10] P. Cox, R. Betts, C. Jones, S. Spall, Acceleration of global warming due to carbon-cycle feedbacks in a coupled climate model, *Nature* 408 (2000) 184–187.
- [11] P. Tans, I. Fung, T. Takahashi, Observational constraints on the global atmospheric CO_2 budget, *Science* 247 (1990) 1431–1438.
- [12] N.A. Owen, O.R. Inderwildi, D.A. King, The status of conventional world oil reserves – hype or cause for concern?, *Energy Policy* 38 (2010) 4743–4749.
- [13] G.V. Chilinger, T.F. Yen, Bitumens, Asphalts, and Tar Sands, Elsevier, 2011.
- [14] P. Atkins, T. Overton, J. Rourke, M. Weller, F. Armstrong, Shriver & Atkins Inorganic Chemistry, fifth ed., Oxford University Press, Oxford, 2010.
- [15] DOE, Targets for Onboard Hydrogen Storage Systems for Light-Duty Vehicles, in Office of Energy Efficiency and Renewable Energy and the FreedomCAR and Fuel Partnership, 2009.
- [16] DOE, Hydrogen Program, in: Hydrogen, Fuel Cells and Infrastructure Technologies Program, Washington, 2011.
- [17] A. Zuttel, Hydrogen storage methods, *Naturwissenschaften* 91 (2004) 157–172.
- [18] P. Bénard, R. Chahine, P.A. Chandonia, D. Cossement, G. Dorval-Douville, L. Lafi, P. Lachance, R. Paggiaro, E. Poirier, Comparison of hydrogen adsorption on nanoporous materials, *J. Alloys Compd.* 446 (2007) 380–384.
- [19] A.W.C. van den Berg, C. Otero-Areán, Materials for hydrogen storage: current research trends and perspectives, *Chem. Commun.* (2008) 668–681.
- [20] H. Xie, Y. Shen, G. Zhou, S. Chen, Y. Song, J. Ren, Effect of preparation conditions on the hydrogen storage capacity of activated carbon adsorbents with super-high specific surface areas, *Mater. Chem. Phys.* 141 (2013) 203–207.
- [21] W.C. Xu, K. Takahashi, Y. Matsuo, Y. Hattori, M. Kumagai, S. Ishiyama, S. Iijima, Investigation of hydrogen storage capacity of various carbon materials, *Int. J. Hydrogen Energy* 32 (2007) 2504–2512.
- [22] H. Jiang, X.-L. Cheng, H. Zhang, Y.-J. Tang, C.-X. Zhao, Molecular dynamic simulation of high-quality hydrogen storage in pillared bilayer graphene bubble structure, *Comp. Theor. Chem.* 1068 (2015) 97–103.
- [23] J. Germain, J. Hradil, J. Fréchet, F. Svec, High surface area nanoporous polymers for reversible hydrogen storage, *Chem. Mater.* 18 (2006) 4430–4435.
- [24] G. Spoto, J.G. Vitillo, D. Cocina, A. Damin, F. Bonino, A. Zecchina, FTIR spectroscopy and thermodynamics of hydrogen adsorbed in a cross-linked polymer, *Phys. Chem. Chem. Phys.* 9 (2007) 4992–4999.
- [25] M. Dincă, A. Yu, J. Long, Microporous metal-organic frameworks incorporating 1,4-benzenedinitrazolate: syntheses, structures, and hydrogen storage properties, *J. Am. Chem. Soc.* 128 (2006) 8904–8913.
- [26] M. Dincă, A. Dailly, Y. Liu, C. Brown, D. Neumann, J. Long, Hydrogen storage in a metal-organic framework with exposed Mn^{2+} coordination sites, *J. Am. Chem. Soc.* 128 (2006) 16876–16883.
- [27] N.L. Rosi, J. Eckert, M. Eddaoudi, D.T. Vodak, J. Kim, M. O'Keefe, O.M. Yaghi, Hydrogen storage in microporous metal organic frameworks, *Science* 300 (2003) 1127–1129.
- [28] P. Georgiev, A. Albinati, B. Mojet, J. Ollivier, J. Eckert, Observation of exceptionally strong binding of molecular hydrogen in a porous material: formation of an $\eta(2)$ -H₂ complex in a Cu-exchanged ZSM-5 zeolite, *J. Am. Chem. Soc.* 129 (2007) 8086–8087.
- [29] X. Solans-Monfort, V. Branchadell, M. Sodupe, C. Zicovich-Wilson, E. Gribov, G. Spoto, C. Busco, P. Ugliengo, Can Cu⁺-exchanged zeolites store molecular hydrogen? An Ab-Initio periodic study compared with low-temperature FTIR, *J. Phys. Chem. B* 108 (2004) 8278–8286.
- [30] F.J. Torres, B. Civalieri, C. Pisani, P. Ugliengo, An Ab Initio periodic study of acidic chabazite as a candidate for dihydrogen storage, *J. Phys. Chem. B* 110 (2006) 10467–10474.
- [31] J. Weitkamp, M. Fritz, S. Ernest, Zeolites as media for hydrogen storage, *Int. J. Hydrogen Energy* 20 (1995) 967–970.
- [32] Z. Yang, Y. Xia, R. Mokaya, Enhanced hydrogen storage capacity of high surface area zeolite-like carbon materials, *J. Am. Chem. Soc.* 129 (2007) 1673–1679.
- [33] P.A. Denis, F. Iribarne, Hydrogen storage in doped biphenylene based sheets, *Comp. Theor. Chem.* 1062 (2015) 30–35.
- [34] L. Zhang, S. Zhang, P. Wang, C. Liu, S. Huang, H. Tian, The effect of electric field on Ti-decorated graphene for hydrogen storage, *Comp. Theor. Chem.* 1035 (2014) 68–75.
- [35] F.J. Torres, B. Civalieri, A. Terentyev, P. Ugliengo, C. Pisani, Theoretical study of molecular hydrogen adsorption in Mg-exchanged chabazite, *J. Chem. Phys. C* 111 (2007) 1871–1873.
- [36] F.J. Torres, J.G. Vitillo, B. Civalieri, G. Ricchiardi, A. Zecchina, Interaction of H₂ with alkali-metal-exchanged zeolites: a quantum mechanical study, *J. Chem. Phys. C* 111 (2007) 2505–2513.

- [37] F.J. Torres, P. Ugliengo, B. Civalleri, A. Terentyev, C. Pisani, A review of the computational studies of proton- and metal-exchanged chabazites as media for molecular hydrogen storage performed with the CRYSTAL code, *Int. J. Hydrogen Energy* 33 (2008) 746–754.
- [38] G. Turnes-Palomino, M.R. Llop-Carayol, C. Otero-Areán, Hydrogen adsorption on magnesium-exchanged zeolites, *J. Mater. Chem.* 16 (2006) 2884–2885.
- [39] S. Bhatia, A. Myers, Optimum conditions for adsorptive storage, *Langmuir* 22 (2006) 1688–1700.
- [40] W. Sliwa, C. Kozłowski, *Calixarenes and Resorcinarenes*, first ed., Wiley-VCH, 2009, ISBN: 35273226392009.
- [41] S.J. Dalgarno, T. Szabo, A. Siavosh-Haghighi, C.A. Deakyn, J.E. Adams, J.L. Atwood, Exploring the limits of encapsulation within hexameric pyrogallol 4 arene nano-capsules, *Chem. Commun.* (2009) 1339–1341.
- [42] S. Manzano, C.H. Zambrano, M.A. Méndez, E.E. Dueno, R.A. Cazar, F.J. Torres, A theoretical study of the conformational preference of alkyl- and aryl-substituted pyrogallol[4]arenes and evidence of the accumulation of negative electrostatic potential within the cavity of their rccc conformers, *Mol. Simul.* 40 (2013) 327–334.
- [43] A.B. Rozhenko, W.W. Schoeller, M.C. Letzel, B. Decker, C. Agena, J. Mattay, Conformational features of calix[4]arenes with alkali metal cations: a quantum chemical investigation with density functional theory, *J. Mol. Struct. – Theochem* 732 (2005) 7–20.
- [44] M. Makinen, P. Vainiotalo, Alkali metal mediated resorcarene capsules: an ESI-FTICRMS study on gas-phase structure and cation binding of tetraethyl resorcarene and its per-methylated derivative, *J. Am. Soc. Mass Spectrom.* 13 (2002) 851–861.
- [45] A.T. Macias, J.E. Norton, J.D. Evansck, Impact of multiple cation- π interactions upon calix[4]arene substrate binding and specificity, *J. Am. Chem. Soc.* 125 (2002) 2351–2360.
- [46] P. Ugliengo, *MOLDRAW: a program to display and manipulate molecular and crystal structures*, Torino, 2006. Available from: <<http://www.moldraw.unito.it>> (cited 2012 Feb 15).
- [47] M.J. Frisch, G.W. Trucks, H.B. Schlegel, G.E. Scuseria, M.A. Robb, J.R. Cheeseman, G. Scalmani, V. Barone, B. Mennucci, G.A. Petersson, H. Nakatsuji, M. Caricato, X. Li, H.P. Hratchian, A.F. Izmaylov, J. Bloino, G. Zheng, J.L. Sonnenberg, M. Hada, M. Ehara, K. Toyota, R. Fukuda, J. Hasegawa, M. Ishida, T. Nakajima, Y. Honda, O. Kitao, H. Nakai, T. Vreven, J.A. Montgomery, J.E. Peralta, F. Ogliaro, M. Bearpark, J.J. Heyd, E. Brothers, K.N. Kudin, V.N. Staroverov, R. Kobayashi, J. Normand, K. Raghavachari, A. Rendell, J.C. Burant, S.S. Iyengar, J. Tomasi, M. Cossi, N.J. Millam, M. Klene, J.E. Knox, J.B. Cross, V. Bakken, C. Adamo, J. Jaramillo, R. Gomperts, R.E. Stratmann, O. Yazyev, A.J. Austin, R. Cammi, C. Pomelli, J.W. Ochterski, R.L. Martin, K. Morokuma, V.G. Zakrzewski, G.A. Voth, P. Salvador, J.J. Dannenberg, S. Dapprich, A.D. Daniels, O. Farkas, J.B. Foresman, J.V. Ortiz, J. Cioslowski, D.J. Fox, *Gaussian 09, Revision A.1.*, Gaussian, Inc., Wallingford, CT, 2009.
- [48] T. Dunning, Gaussian basis sets for use in correlated molecular calculations. I. The atoms boron through neon and hydrogen, *J. Chem. Phys.* 90 (1989) 1007.
- [49] S.F. Boys, F. Bernardi, The calculation of small molecular interactions by the differences of separate total energies. Some procedures with reduced errors, *Mol. Phys.* 100 (2002) 65–73.
- [50] B. Lindberg, A new efficient method for calculation of energy eigenvalues and eigenstates of the one-dimensional Schrodinger equation, *J. Chem. Phys.* 88 (1988) 3805–3810.
- [51] R. Dovesi, R. Orlando, A. Erba, C.M. Zicovich-Wilson, B. Civalleri, S. Casassa, L. Maschio, M. Ferrabone, M. De La Pierre, P. D'Arco, Y. Noel, M. Causa, M. Rerat, B. Kirtman, CRYSTAL14: a program for the Ab Initio investigation of crystalline solids, *Int. J. Quant. Chem.* 114 (2014) 1287–1317.
- [52] R. Dovesi, V.R. Saunders, C. Roetti, R. Orlando, C.M. Zicovich-Wilson, F. Pascale, B. Civalleri, K. Doll, N.M. Harrison, I.J. Bush, P. D'Arco, M. Llunell, M. Causa, Y. Noel, CRYSTAL14 User's Manual, fifth ed., University of Torino, Torino, Italy, 2014.
- [53] S. Tosoni, F. Pascale, P. Ugliengo, R. Orlando, V.R. Saunders, R. Dovesi, Vibrational spectrum of brucite, Mg(OH)₂: a periodic ab initio quantum mechanical calculation including OH anharmonicity, *Chem. Phys. Lett.* 396 (2004) 308–315.
- [54] P. Ugliengo, ANHARM: A Program to Solve the Mono Dimensional Nuclear Schrodinger Equation, University of Torino, Torino, Italy, 1989.
- [55] Y. Zhao, D.G. Truhlar, Density functionals with broad applicability in chemistry, *Acc. Chem. Res.* 41 (2008) 157–167.
- [56] S. Grimme, Semiempirical GGA-type density functional constructed with a long-range dispersion correction, *J. Comput. Chem.* 27 (2006) 1787–1799.
- [57] S. Grimme, Semiempirical hybrid density functional with perturbative second-order correlation, *J. Chem. Phys.* 124 (2006) 034108.
- [58] S. Grimme, J. Antony, S. Ehrlich, H. Krieg, A consistent and accurate ab initio parameterization of density functional dispersion correction (DFT-D) for the 94 elements H-Pu, *J. Chem. Phys.* 132 (2010) 154104.
- [59] S. Grimme, S. Ehrlich, L. Goerigk, Effect of the damping function in dispersion corrected density functional theory, *J. Comput. Chem.* 32 (2011) 1456–1465.
- [60] S. Dapprich, I. Komaromi, K.S. Byun, K. Morokuma, M.J. Frisch, A new ONIOM implementation in Gaussian98. Part I. The calculation of energies, gradients, vibrational frequencies and electric field derivatives, *J. Mol. Struct. – Theochem* 461 (1999) 1–21.
- [61] C. Møller, M. Plesset, Note on an approximation treatment for many-electron systems, *Phys. Rev.* 46 (1934) 618.
- [62] I. Roggero, B. Civalleri, P. Ugliengo, Modeling physisorption with the ONIOM method: the case of NH₃ at the isolated hydroxyl group of the silica surface, *Chem. Phys. Lett.* 341 (2001) 625–632.
- [63] M. Kocman, P. Jurecka, M. Dubecky, M. Otyepka, Y. Cho, K.S. Kim, Choosing a density functional for modeling adsorptive hydrogen storage: reference quantum mechanical calculations and a comparison of dispersion-corrected density functionals, *Phys. Chem. Chem. Phys.* 17 (2015) 6423–6432.